Unusual Dependence of Particle Architecture on Surfactant Concentration in Partially Fluorinated Decylpyridinium Templated Silica

Bing Tan,[†] Sandhya M. Vyas,[‡] Hans-Joachim Lehmler,[‡] Barbara L. Knutson,[†] and Stephen E. Rankin*[,†]

Chemical and Materials Engineering Department, University of Kentucky, 177 Anderson Hall, Lexington, Kentucky 40506-0046 and Department of Occupational and Environmental Health, University of Iowa, 100 Oakdale Campus #124 IREH, Iowa City, Iowa 52242-5000

Received: July 29, 2005; In Final Form: October 20, 2005

A series of porous silica particles is prepared with different concentrations of the fluorinated cationic surfactant 1-(3,3,4,4,5,5,6,6,7,7,8,8,9,9,10,10,10)-heptadecafluorodecyl)pyridinium chloride (HFDePC) to trace the changes in pore structure and particle morphology as the surfactant concentration increases. At the lowest concentration studied (1.5 mmol/L), the product consists of small round particles with close-packed cylindrical mesopores. As the HFDePC concentration increases, macroporous voids are introduced to create multi-chambered hollow particles with mesoporous walls. With a still higher concentration of HFDePC the macropore volume decreases, and elongated, tactoid-like nanoparticles are formed with random mesh-phase pores oriented with silica layers perpendicular to the main axis of the particles. Further increasing the concentration of HFDePC eventually leads to the formation of round particles with disordered pores. These changes are consistent with increasing HFDePC concentration favoring increasingly oblate or disklike micelles. The process of forming the elongated particles with random mesh-phase structure is investigated by TEM of chilled and dried samples. The results indicate that the oriented tactoid-like structure forms spontaneously within 2 min by co-assembly of silica and HFDePC rather than by preferred growth perpendicular to the layers. The particle shape and layer orientation are consistent with what would be expected for a liquid-crystal particle with orientation-dependent surface tension. Finally, we compare samples prepared with a high HFDePC and with good or poor mixing. With inadequate mixing, a gel layer forms at the top of the sample which is composed of elongated mesoporous particles with a thick coating of microporous silica. The lower particulate phase contains small disordered particles similar to those obtained in a well-mixed sample. Presumably, the structure of the upper layer results from initial immiscibility of the precursor and slow diffusion of silicates out of the gel.

Introduction

Fluorinated surfactants are highly surface-active analogues of conventional hydrocarbon surfactants.[1] The replacement of hydrogen with fluorine in the tails of these surfactants makes them very hydrophobic, somewhat lipophobic, and, in some cases, biologically inert.[2] The large cross-sectional area and stiffness of fluorocarbons favors micellar aggregates with low curvature (such as disks, bilayers, and tubules) and unusual intermediate phases such as mesh-phases.[2−6]

Because of their unusual self-assembly behavior, fluorinated surfactants have recently begun to be explored as templates for the synthesis of nanoporous ceramics.[7−12] Their intermolecular interactions and phase behavior may lead to new pore and particle structures, controlled organic functionalization,[13] and processing with low-surface-tension fluids such as compressed CO_2.[14] Blin and co-workers determined the phase diagram of $F(CF_2)_8C_2H_4(OC_2H_4)_9OH$ in water and used the phase diagram to guide the formation of silica with hexagonal mesopores.[9] We have demonstrated that with a homologous series of 1H,1H,2H,2H-perfluoroalkylpyridinium chloride templates, the variety of pore structures obtained is greater than that obtained with hydrocarbon surfactants.[11] Particles with low-curvature pores (slit-shaped or lamellar) are formed using surfactants with the longest tails, which is consistent with the self-assembly behavior of these surfactants.[7,11]

One member of the series of fluorinated cationic surfactants that we have used, 1-(3,3,4,4,5,5,6,6,7,7,8,8,9,9,10,10,10-heptadecafluorodecyl)pyridinium chloride (HFDePC), has been shown to display interesting phase behavior in aqueous solution.[5] Like other fluorinated surfactants, it can readily form mesh-phases[5] which are only rarely found in hydrogenated surfactant systems.[15,16] When used as a pore template, HFDePC forms novel particles by room-temperature precipitation, namely, cigar-shaped particles with random mesh-phase pores[7] and hollow vesicle-like particles with mesoporous shells.[12] The initial surfactant concentration leading to the vesicle-like structure is lower than that leading to the random mesh-phase structure. This order of structures is unusual. When a cationic hydrogenated surfactant such as CTAB acts as the template, the usual pore structure trend is from wormhole-like to hexagonal to lamellar as the surfactant concentration increases.[17,18] Under certain circumstances, bicontinuous cubic structures with space group *Ia*3*d* form at conditions between those giving hexagonal and lamellar structures.[17,18] Here, we study the architectures of HFDePC templated silica particles as a function of concentra-

* Author to whom correspondence should be addressed. Telephone: (859) 257-9799. E-mail: srankin@engr.uky.edu.
[†] University of Kentucky.
[‡] University of Iowa.

10.1021/jp054219h CCC: $30.25
Published on Web 11/19/2005

tion, with the goal of understanding how to access and control their unusual structures.

We will describe the preparation of a series of samples with the only difference being the surfactant concentration. First, we will describe the synthesis and characterization of a series of samples prepared in well-mixed aqueous solutions. We will be particularly interested in the transition from vesicle-like hollow structures to elongated particles with mesh-phase pores. A highly unusual sequence from close-packed cylinders to vesicular particles to mesh-phase to disordered particles is observed. We will examine the mechanism of forming these structures by TEM of cold-dried samples withdrawn from the synthesis solutions. The results show that these structures form spontaneously during the co-assembly of the silica−surfactant aggregates, rather than forming through asymmetric growth processes. Finally, we will comment on segregated structures that can form if the mixing is inadequate.

Experimental Section

Materials. The fluorinated surfactant HFDePC was synthesized as described previously by alkylation of anhydrous pyridine with $C_8F_{17}C_2H_4I$ followed by anion exchange.[19] Tetraethoxysilane (TEOS, 98%) was obtained from Sigma. Concentrated aqueous ammonia (29 wt % NH_4OH, Merck), deionized ultrafiltered water, concentrated aqueous HCl (ACS grade, Fisher Scientific), and anhydrous ethanol (Aaper Alcohol and Chemical) were used for materials synthesis.

Materials Syntheses. The synthesis procedure was similar to the procedure reported previously.[7] Because of the limited quantity of surfactant, smaller samples were prepared for the most concentrated solutions. To ensure that the size of the reactor vessel and the scale of solution did not influence the results, two series of samples were prepared in different batch sizes, but with all variables held constant except the concentration of HFDePC. For the first series, samples 1 to 3 were prepared with initial compositions of *x* g HFDePC:112 g water:6.14 g concentrated aqueous ammonia:8.72 g TEOS. The variable *x* was equal to 0.1, 0.14, and 0.78 for samples 1 through 3, respectively. The size of the beaker, the stir bar, stirring speed, and TEOS addition speed were kept the same among these macroscopically well-mixed samples. The second series of samples, samples 4 to 8, was prepared with initial compositions of *x* g HFDePC:12.44 g water:0.68 g concentrated aqueous ammonia:0.97 g TEOS. *x* was 0.087, 0.23, 0.3, 0.5, and 0.8 for samples 4 through 8, respectively. The synthesis conditions were the same among these samples. A fast stirring speed was used for all samples to obtain homogeneous solutions. From the two series, a pair of samples (samples 3 and 4) with identical composition was prepared to confirm that the reactor scale did not influence the results. The ingredients were mixed in the reverse order listed and aged for 24 h before filtering and drying. The surfactant was extracted from each sample using an acidic ethanol/water solution, as described previously.[7]

When the concentration of cationic fluorinated surfactant was highest (sample 8), extensive phase separation was observed after aging. A fast stirring speed had to be used to obtain a homogeneous solution. To illustrate the importance of mixing, one additional sample was prepared with the same recipe as sample 8 but with a larger volume of solutions, so that the entire sample was not completely mixed at all times. The top of the resulting product solution was a soft gel, while the bottom remained fluid. After aging for 24 h, the gel layer (sample 8ST) was separated from the bottom fluid layer (sample 8SB). Both samples were filtered and the surfactant was extracted.

Characterization. X-ray diffraction (XRD) patterns were recorded with a Siemens 5000 diffractometer using Cu Kα radiation. Diffraction data were recorded between 1.5° and 10° with a step size of 0.02° and a scanning speed of 0.008 degrees/min. Transmission electron microscope (TEM) images were collected with a JEOL 2010F electron microscope operating at 200 kV. Nitrogen sorption measurements were performed using a Micromeritics Tristar 3000 system. All samples were degassed at 120 °C for 4 h under flowing nitrogen prior to measurement. The BJH method with a modified statistical film thickness equation[20] was used to calculate the pore size distributions from the adsorption branch of the isotherms. The pores in all samples were assumed to have cylindrical cross sections to allow for comparison.

Results and Discussion

In a cationic hydrogenated surfactant templated sol−gel process, precipitates are usually obtained within several minutes after the addition of TEOS.[21] This differs from templating with a cationic fluorinated surfactant, in which the resulting silica particles formed by TEOS often are suspended colloids instead of precipitates. This indicates either that condensation is not as extensive as with a hydrogenated surfactant, or that small particles are stabilized by fluorinated surfactants. A lower extent of condensation might be reached because, while interactions between silicate anions and cationic surfactants are sufficient to induce particle formation, repulsion between the silicate species and the surfactant tails may delay or prevent hydrolysis and condensation. On the other hand, the small particle size may be dictated by the high surface activity of the fluorinated surfactant.[22]

Because of the contradictory interactions between the silicate species and the head or tail of the fluorinated chains, the pore properties and particle morphology can be unusually sensitive to the process conditions. Investigations in our laboratory have shown that the pore properties of these materials are sometimes affected by stirring speed, TEOS addition speed, amount of solution, and reactor size. The drying conditions also influence the pore properties. The effect of different stirring speeds on the particle morphology was previously investigated for vesicle-like particles prepared using HFDePC.[12] With very slow stirring, single-walled vesicle-like silica particles are obtained. Increasing the stirring speed leads to agglomeration of the vesicles into elongated multi-chambered particles with porous shells. Here, the stirring rate is kept high enough that all samples except 8S appear macroscopically well-mixed. As described above, samples 1−3 are prepared in larger batches than samples 4−8, but samples 3 and 4 have identical compositions to ensure that the difference in batch size does not affect the results. The concentrations of all reactants except HFDePC are kept constant for all samples.

Transition from Close-Packed Cylindrical Pores to Vesicle-Like Particles. Representative TEM images of samples 1 through 3 are compared in Figure 1. Sample 1, prepared with the lowest concentration of HFDePC, consists of uniform mesoporous particles with close-packed cylindrical pores. Most particles in this sample are found to be round (somewhat deformed spheres) by TEM. Both stripe and spot patterns are observed, corresponding to views across and along close-packed cylindrical pores, respectively. As illustrated by the particles in the lower left corner of Figure 1, the cylindrical pores are highly curved due to the small particle size. The spot pattern in the upper right particle in the leftmost panel of Figure 1 is not a perfect 2D hexagonal pattern, but instead is compressed in one direction, similar to a rectangular phase.[23]

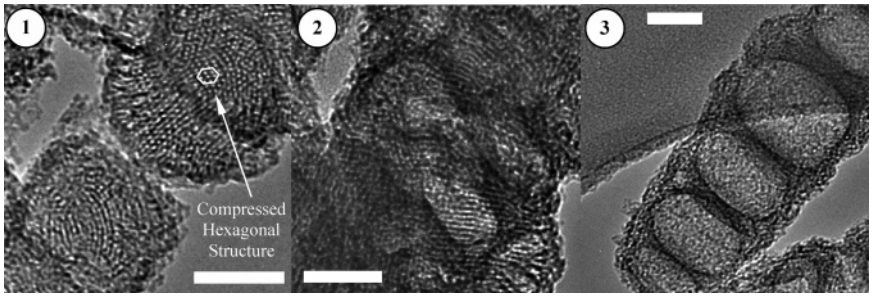

Figure 1. Representative TEM images for samples 1−3. The scale bars are all 50-nm wide. The hexagon indicates the deformed hexagonal unit cell of the pores.

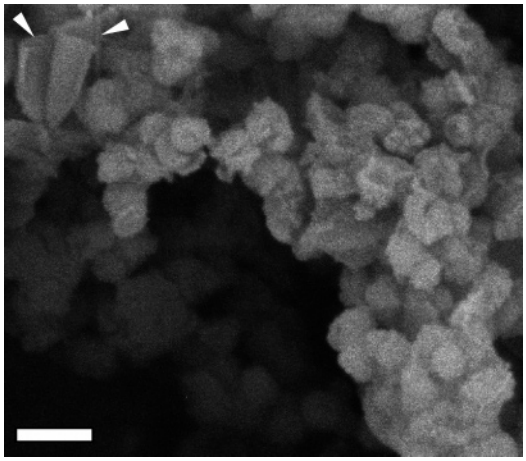

Figure 2. Representative SEM image of sample 1. The white arrows indicate sheetlike structures found infrequently in this sample. The scale bar is 250-nm wide.

Increasing the HFDePC concentration by 40% in sample 2 leads to particles containing hollow cells (macropores). These hollow cells appear to have been captured within larger solid particles. Ordered patterns (stripes in Figure 1) are still evident in the walls of this sample. The particles in sample 2 are larger and more elongated compared to those in sample 1. Sample 3 consists of particles which are more elongated yet and which have multiple distinct hollow cells arranged along their axes. No long-range order is found in the shell walls, but they are mesoporous. In our initial study of this system, the elongated particles with hollow cells were shown to be formed by coalescence of individual vesicle-like hollow silica particles.[12] Thus in this series, TEM suggests that at the lowest HFDePC concentration the product has defective close-packed cylindrical pores, and increasing the concentration of HFDePC gradually induces the co-assembly of silica and HFDePC into hollow, vesicle-like structures which coalesce into elongated particles.

The change of the particle shape inferred from the TEM images is confirmed by SEM. Most of the particles in sample 1 are rough round particles under SEM (Figure 2). Sheetlike particles are also found in the SEM images (indicated with white arrows in Figure 2), but they are much rarer than the round particles. Elongated particles are confirmed in sample 3 by SEM, similar to those described in the initial report on vesicle-like particles prepared with HFDePC.[12]

The XRD patterns that were collected for samples 1−3 exhibit no reflections. This is consistent with the small particle size and highly curved pore structures observed by TEM. The absence of reflections shows that there are no large, well-ordered domains in these samples, despite the close-packed order found in samples 1 and 2 by TEM.

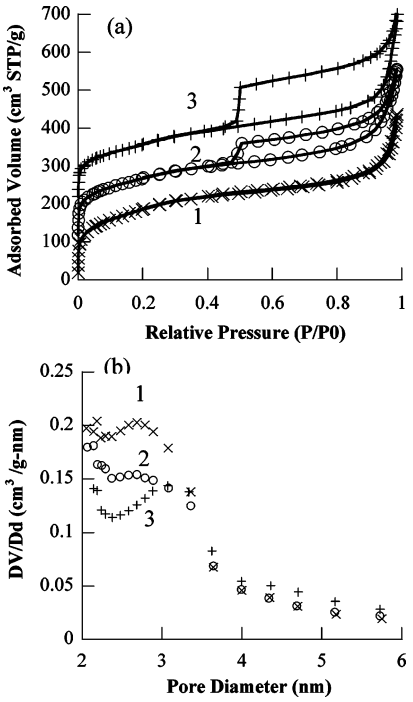

Figure 3. Nitrogen sorption isotherm plots (a) of samples 1, 2 (upshifted 100 cm^3/ g), and 3 (upshifted 200 cm^3/g). (b) Calculated pore size distributions of the first three samples.

Nitrogen sorption isotherm plots of the first three samples are shown in Figure 3. All three samples have weak inflections indicating the presence of uniform mesopores. Type H3 hysteresis loops are observed for samples 2 and 3.[24] This type of hysteresis is associated with large meso- or macropores surrounded by walls with smaller meso- or micropores. This interpretation is consistent with the hollow cells observed inside of the particles in Figure 1. The hysteresis of sample 3 is larger than that of sample 2, which is consistent with a larger number of hollow cells in this sample. The mesopore size distributions for the three samples show pores of consistent diameter (∼2.8 nm for samples 1 and 2, and ∼3.2 nm for sample 3) and a decrease in mesopore volume as more hollow cells are produced in this series.

Transition from Vesicle-Like Particles to Mesoporous Tactoids and Spheres. Representative TEM images for samples 5 through 8 are shown in Figure 4. The elongated particles with multiple hollow cells found for sample 4 (TEM not shown) are consistent with those of Sample 3, which was prepared from the same composition in a larger batch. As the concentration of HFDePC increases, elongated particles with fewer hollow cells are observed in sample 5. In sample 6, only uniform mesoporous elongated particles (tactoids) with silica layers oriented perpendicular to the particle axis are observed. This

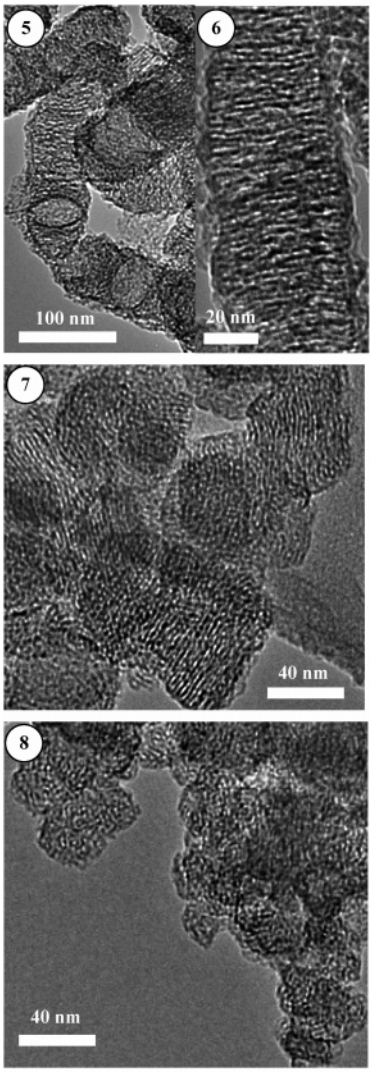

Figure 4. Representative TEM images of samples 5−8.

pattern was previously identified as a random mesh-phase structure.[7] No hollow cells are apparent in this sample. In sample 7, a layered pattern is still observed, but the particles are shorter than those in sample 6. A disordered pore structure is observed for sample 8. The particles in this sample are aggregates of small round nanoparticles. The particle sizes in this sample are noticeably smaller than those in sample 7.

SEM images of samples 4 through 6 confirm that these samples consist of elongated particles.[7,12] SEM images of samples 7 and 8 (Figure 5) show that both of the samples are made up of rough spherical particles. These spherical particles are flocculated into large aggregates. Smaller particles are observed in sample 8 than in sample 7. These observations are consistent with the TEM findings.

XRD patterns were collected for samples 4 through 8. Two reflections with a *d* spacing ratio of 2:1 were observed in the XRD patterns of samples 6 and 7. This pattern is consistent with a lamellar pore structure with randomly arranged pillars between adjacent silica layers. This structure is the same as the random mesh-phase pore structure described before.[7] The lack of a weak low-angle peak representing scattering from pillars within the pore layers may be due to poor ordering of the pillars in the samples prepared under the current conditions. While there is no reflection from the pillars, the stability of the layers to surfactant removal demonstrates that the layers are pillared, as in a random mesh phase. No reflections are observed for sample

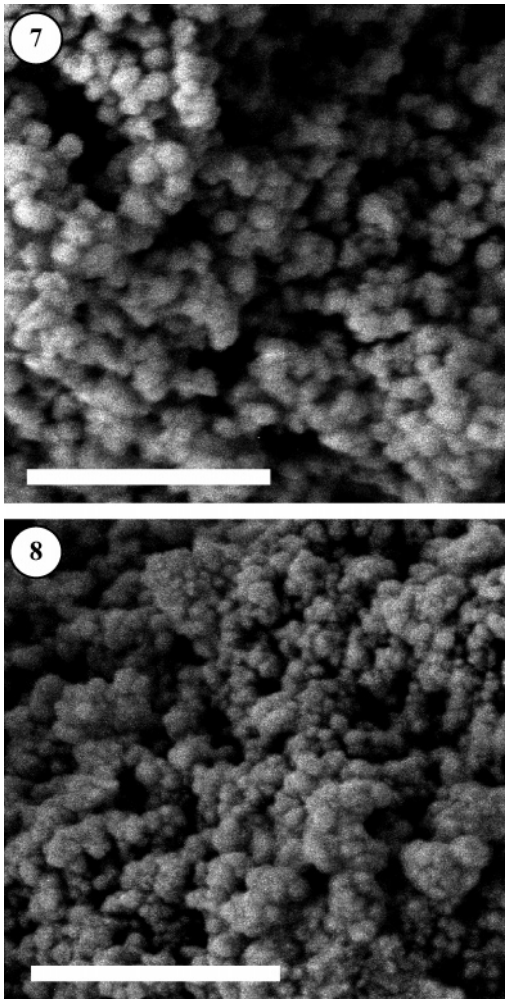

Figure 5. Representative SEM images of samples 7 and 8. The scale bars are 750-nm wide.

8 either before or after extraction. This is consistent with the disordered pore structure observed by TEM.

Nitrogen sorption isotherm plots and pore size distributions of samples 4−8 are compared in Figure 6. Sample 4 has an isotherm similar to that of sample 3. Both isotherms have large H3 hysteresis loops indicating the presence of a large number of hollow cells. As the HFDePC concentration increases in this series, the hysteresis loop disappears, and textural porosity is indicated by the upturn at high relative pressure. The pore size distributions of all samples indicate comparable pore sizes (∼3.2 nm), but the mesopore volume increases significantly on going from sample 4 to sample 7. The mesopore volume declines again in sample 8 due to its disordered pore structure. With the increase of HFDePC in this series, the evolution of the pore structure and particle morphology is the reverse of the trend for samples 1−3. Vesicle-like hollow cells are gradually lost from the elongated particles in this series as a mesh phase becomes preferable. As the HFDePC concentration increases further, the elongated particles shorten into round particles.

Cold-Dried TEM Specimens. Of all the particle morphologies observed, the elongated mesh-phase structures (e.g., sample 6) are the most difficult to rationalize in terms of known mesopore architectures. The orientation of the layers of the mesh phase perpendicular to the particle axis may be explained either by the preferential growth of the particles perpendicular to existing layers, or by the structure that is thermodynamically favored in a liquid-crystal dispersion. To better understand their formation mechanism, we examined cold-dried TEM samples.

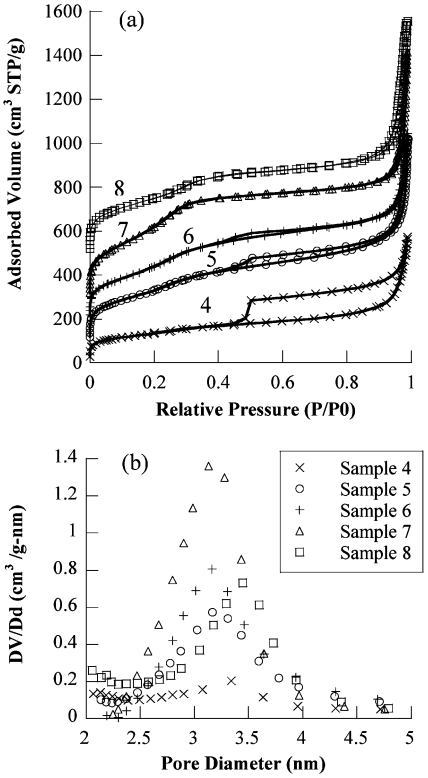

Figure 6. Nitrogen sorption isotherm plots (a) of samples 4, 5 (upshifted 100 cm^3/ g), 6 (upshifted 200 cm^3/g), 7 (upshifted 300 cm^3/ g), and 8 (upshifted 500 cm^3/g). (b) Calculated pore size distributions of all samples.

These samples were prepared by placing a drop of solution onto a liquid-nitrogen-chilled (−2 °C) lacey carbon TEM grid resting on a lint-free absorbent tissue. The solution was quickly thinned by capillary suction of solvent into the tissue and subsequently dried by forced air. All samples were observed in the TEM instrument within 4 h of preparation. Although we are aware that drying artifacts may influence the results, we have previously been able to observe the development of micelle ordering in precipitated particles by this method.[25]

Four specimens were prepared by withdrawing aliquots of the synthesis solution of sample 6 after 30 s, 2 min, 4 min, or 8 min of reaction. The results are shown in Figure 7. After 30 s, surfactant−silica aggregates are present in the sample. A few silica vesicles are identified as well as a large number of uniform particles without any defined shape (not shown). No ordered surfactant aggregates are observed at this time. The presence of a small number of vesicular particles seems to be temporary, because no vesicle-like structures are identified in the corresponding product. The structures isolated after 30 s must be soft enough to re-organize. In the next sample withdrawn (2 min, Figure 7), elongated particles with weak density contrast could already be observed. Layers can be identified in each of the weakly condensed particles, which are oriented perpendicular to the particle axis. The density contrast of the particles increases in the TEM sample isolated after 4 min due to increasing silica condensation. The particles are more clearly cigar-shaped, with surfactant layers oriented perpendicular to their long axes. Particles collected after 8 min are still elongated, but the micelle structure is difficult to resolve. The difficulty in seeing the structure is most likely due to the low contrast between highly condensed silica and the fluorinated surfactant micelles. This experiment shows that the unusual orientation of the micelle layers perpendicular to the axis of these elongated particles

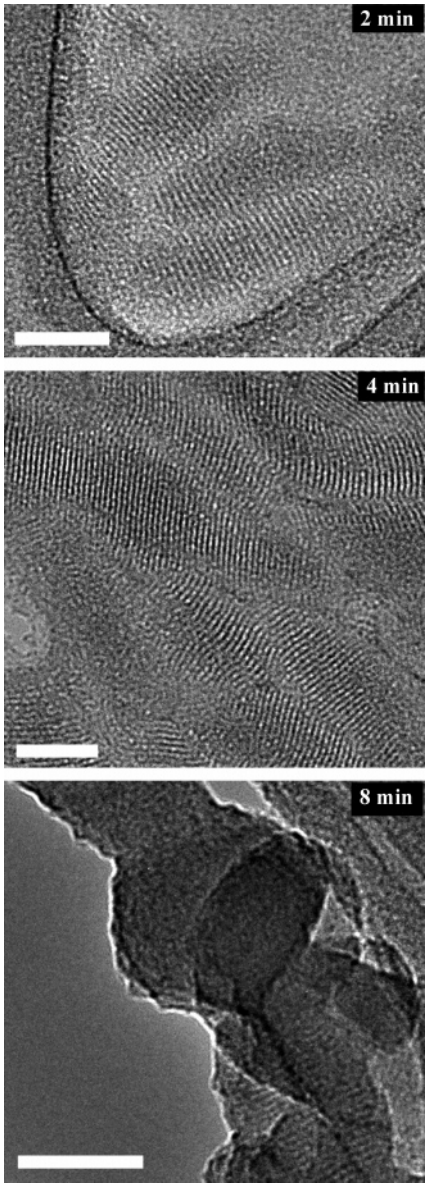

Figure 7. TEM images of cold-dried specimens of the solution giving sample 6 collected 2 min, 4 min, and 8 min after adding TEOS. The scale bars are 50-nm wide.

emerges suddenly after precipitation of the particles and only becomes more fully condensed with time. The elongated structure does not form by anisotropic growth, as we originally hypothesized.[7] The elongated shape of the particles must simply be the thermodynamically favorable shape for this ordered, heterogeneous structure.

The same cold-drying procedure was also applied for samples 1 and 4 to learn more about how their structures develop. No ordered structure was observed for either sample in the dried TEM specimens withdrawn after 2 or 4 min. For sample 1, a slow rate of TEOS hydrolysis probably makes it difficult to isolate an ordered specimen with adequate electron density contrast for TEM. For sample 4, the structures may initially be too delicate to withstand drying. Only after 8 minutes of reaction of sample 4 is the specimen stable enough to be able to isolate hollow structures similar to those of the final product. Thus, for all of the cold-dried TEM samples, we were unable to isolate any ordered intermediate structures. The final particle architectures are the first organized structures that we can identify. Prior to the appearance of these structures, only disordered

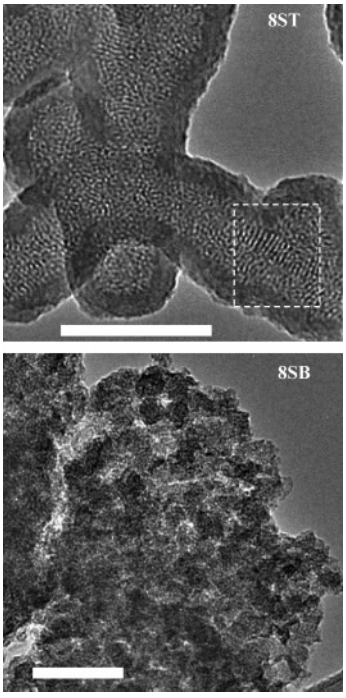

Figure 8. Representative TEM images of samples 8ST and 8SB. The scale bars are 100-nm wide. A layered pattern is outlined with a rectangle for sample 8ST.

aggregates can be identified. This suggests that the mechanism of formation of the observed structures in all cases is thermodynamically driven co-assembly of silicate−surfactant aggregates, rather than selective growth processes.

Effects of Inadequate Stirring. As we mentioned earlier, it was important to use a high stirring rate for all of the samples to ensure a homogeneous distribution of reactants. Because fluorocarbons are both hydrophobic and lipophobic, TEOS is not as readily dissolved and hydrolyzed as it is with hydrocarbon surfactants. Therefore, process parameters such as stirring rate can influence the outcome of the process. Previously, we reported that stirring can induce aggregation of individual vesicle-like particles into particles with multiple hollow cells similar to those of sample 3.[12] In some of the more concentrated solutions investigated here, gels can be obtained when the stirring rate is too low to homogenize the solution. To investigate the effect of inefficiency of stirring on the pore structure, sample 8S was prepared with the same composition as sample 8, but with a larger amount of reactants (and therefore less effective mixing). The top of the solution formed a gel, while the bottom was a colloidal dispersion. The layers were separated, filtered, and the surfactant was extracted from each.

TEM images of these two samples are shown in Figure 8. The sample from the top (8ST) contains uniform elongated mesoporous particles as well as a few hollow spherical particles. Both types of particles are coated with thick shells of amorphous silica. These particles appear similar to the types of particles obtained with lower HFDePC/Si ratios[7,12] except that they have been coated with amorphous silica. The sample from the bottom of the vessel (8SB) is composed of very small particles with disordered pores. The particle morphology is similar to that of sample 8.

The cause of the separation of the sample into two types of structures is likely to be the initial insolubility of the precursor, TEOS. Because TEOS has a density of 0.933 g/mL, it preferentially moves to the top of the solution until it is hydrolyzed. Therefore, near the top, the local ratio of HFDePC/Si is lower than the overall ratio. This leads to a distribution of both uniform and hollow mesoporous silica particles. The elongated colloidal particles easily gel because the top of the solution is not strongly sheared. After the gel forms, the remaining TEOS is not able to easily diffuse away, and instead it deposits to form the amorphous silica coating. The lower layer, on the other hand, is well mixed and has a high HFDePC/Si ratio, which leads to a structure similar to that of the well-mixed sample 8. The comparison of samples 8ST and 8SB shows that the stirring speed is critical to control the product quality in situations where the TEOS is slowly hydrolyzed and not readily miscible with the surfactant. The importance of mixing also explains why a few vesicles were observed after 30 s in the cold-dried TEM specimen of sample 6. These vesicles may have formed initially due to insufficient mixing of TEOS oil droplets. A low local HFDePC/Si ratio may have caused these vesicles to form. However, the condensation at this stage was weak enough that the vesicles reorganized into uniform mesh-phase particles with continued stirring. If the stirring was slower, vesicles would probably have been obtained, similar to those observed in sample 8ST.

Discussion of the Pore Structure Sequence. To summarize the observations of HFDePC templated silica, the first sample consists of uniform particles with close-packed cylindrical mesopores. The concentration of HFDePC prior to adding TEOS (1.5 mmol/L) is less than the cmc of the surfactant (2.6 mmol/L).[26] This indicates that silica−surfactant co-assembly is strong enough to induce micellization and ordering. The micelles are packed into a slightly compressed 2D hexagonal lattice (similar to a rectangular phase), which indicates that the cross section of the micelles may be somewhat asymmetrical.

As the concentration of surfactant is first increased (samples 1 to 3), hollow vesicle-like structures are favored. This is consistent with the tendency of fluorinated surfactants to form low-curvature structures such as disk micelles and bilayers.[3,4,21] We know that sample 1 is formed from cylindrical pores and that sample 6 is formed from disk or fragmented bilayer micelles. Between, the HFDePC micelles must pass through a cylinder-to-disk transition. This type of transition is common for fluorinated surfactants in the presence of salts,[2,4,6] due to the larger tail cross-sectional area and stiffness of fluorinated surfactants.[6,27,28] This micelle shape transition is also consistent with the hexagonal to rectangular to mesh-phase sequence of phases in the HFDePC/water-phase diagram.[5] This transition should involve the micelles first becoming more ribbonlike and then breaking up into shorter ribbons and disks. The vesicle-like structures found in samples 2 and 3 can be rationalized on the basis of two effects. First, silica would be expected to aggregate preferentially with the flatter surfaces of the micelles (where the headgroup density is highest). For micelles that are only somewhat flattened, this leads to co-assembly of HFDePC micelles and silica into sheets, which further organize into vesicle-like particles. Second, the flattened micelles may be stiffer than cylinders, which provides a driving force to reduce their amount of curvature by forming vesicle-like hollow aggregate rather than close-packed cylinders confined in small particles (as in sample 1). The increasing disorder in the walls of sample 3 compared to those of sample 2 is also consistent with a cylinder-to-disk transition which disrupts the packing of the micelles. The disorder in the walls may also be increased during the aggregation of several vesicle-like aggregates into elongated particles with multiple hollow cells.

As the surfactant concentration increases further (samples 4 to 7), hollow cells are lost in favor of mesh-phase-like pillared

lamellar mesopores. This is consistent with the HFDePC micelles becoming more disklike as the concentration increases. Continued preference for silicates at the flatter faces of the micelles would favor structures with more layering, such as the observed mesh-phase structure. The layers in the particles are organized into elongated particles in which the surfactant layers are perpendicular to the long axis of the particles. The formation of such tactoids is a well-known phenomenon in liquid-crystal dispersions.[29] A lamellar structure at an interface with an isotropic medium that has no strong preference for either layer would have a lower interfacial energy when the layers are oriented perpendicular to the interface than when they are parallel.[30] Wulff showed that the orientation-dependent surface tension of a layered structure gives rise to elongation in the direction perpendicular to the layers.[31] This is precisely what we see in sample 6, and similar shapes have been recently shown to be favorable in small droplets of nematic[32] and smectic[33] liquid crystals. According to this explanation, the reason that sample 7 consists of particles with a smaller aspect ratio than that of sample 6 may be either (a) an increase in surface tension or (b) a decreased tendency for the liquid-crystal director (in this case, the orientation of the surfactants) to align parallel to the droplet surface. [32] Either of these changes could result from the aggregation of HFDePC into larger micelles which interact more strongly with silica.

The logical conclusion of this trend would be for the HFDePC to organize into perfect bilayers at the highest concentration. The binary HFDePC/water system passes from a mesh phase to a lamellar phase as the HFDePC concentration increases.[5] We found no evidence for formation of a lamellar structure, but the concentration did become high enough to allow a disordered bicontinuous pore structure to form (sample 8).

The unusual sequence of pore structures observed here is probably a consequence of the ability of this particular surfactant to organize into different types of micelles. The next-shortest surfactant in this series, $C_6F_{13}C_2H_4Py^+ \cdot Cl^-$, does not form materials with this much structural variety. 2D hexagonal close-packed cylindrical pores are observed across a wide surfactant concentration range from below the cmc to well above.[34] On the other hand, the next-longest surfactant, $C_{10}F_{21}C_2H_4Py^+ \cdot Cl^-$, strongly favors bilayers, and it was therefore found to be difficult to form an ordered pore structure at any concentration.[11] Hydrocarbon surfactants tend to undergo a transition directly from cylindrical micelles to bilayers (including bicontinuous cubic intermediate phases), which leads to the usual hexagonal to cubic to lamellar order of phases. The ability of HFDePC to form more oblate or disklike micelles as concentration increases may explain the observed hexagonal to vesicle-like to mesh-phase to disordered bicontinuous pore structure sequence. The corresponding change in particle morphology is apparently dictated by how the silicates and micelles co-assemble and the thermodynamics of the dispersed aggregates.

Conclusions

A series of silica particles was prepared by precipitation from aqueous ammonia with different HFDePC/Si ratios. As this ratio increased, the pore structure changed from hexagonal cylinders to vesicle-like to random mesh phase to disordered bicontinuous pores. The corresponding particle morphology changed from uniform round mesoporous particles to hollow elongated particles to uniform elongated particles to uniform round particles, respectively. This is the first time that we are aware that this sequence of structural transformations has been reported for a surfactant-templated sol−gel process. Using cold-dried TEM specimens of samples withdrawn from the reaction synthesis solution, the formation mechanism of elongated particles with random mesh-phase structure was investigated. Elongated particles with highly ordered layers form quickly by co-assembly of silica and HFDePC, rather than by anisotropic growth of the particles. This indicates that the unusual arrangement of slit-shaped pores perpendicular to the long axis of the particles is the thermodynamically favorable shape of the particles, which can be explained on the basis of the well-known tactoid shape of dispersed droplets of layered liquid crystals.[31,32] The other types of particle structures could not be isolated as easily as cold-dried samples, but we found no indication of any intermediate ordered structure prior to the formation of the hollow vesicle-like particles, which suggests that they also form directly as stable aggregates. The observed pore structure sequence is consistent with a gradual cylinder-to-disk-to-bilayer micelle transition, with the particle morphology following from the silicate−surfactant aggregate structure. Finally, for the sample with the highest HFDePC/Si ratio, we found that because the surfactant does not emulsify TEOS readily, insufficient stirring caused the formation of layers of sample with different structures. The upper layer has a lower HFDePC/Si ratio and contains particles with mesh-phase and vesicle-like structures. The lower layer has a higher HFDePC/Si ratio and contains disordered mesoporous particles similar to what one would expect on the basis of the bulk HFDePC concentration. Although a fluorinated surfactant such as HFDePC produces radically different types of structures than hydrocarbon surfactants do, we can understand the structures formed on the basis of a cylinder-to-disk transition and the behavior of liquid-crystal dispersions.

References and Notes

(1) Hoffmann, H.; Wurtz, J. *J. Mol. Liq.* **1997**, *72*, 191.
(2) Krafft, M. P.; Riess, J. G. *Biochimie* **1998**, *80*, 489.
(3) Boden, N.; Harding, R.; Gelbart, W. M.; Ohara, P.; Jolley, K. W.; Heerdegen, A. P.; Parbhu, A. N. *J. Chem. Phys.* **1995**, *103*, 5712.
(4) Kunze, B.; Kalus, J.; Boden, N.; Brandao, M. S. B. *Physica B* **1997**, *234−236*, 351.
(5) Wang, K.; Oraedd, G.; Almgren, M.; Asakawa, T.; Bergensthl, B. *Langmuir* **2000**, *16*, 1042.
(6) Srinivasan, V.; Blankschtein, D. *Langmuir* **2005**, *21*, 1647.
(7) Tan, B.; Dozier, A.; Lehmler, H.-J.; Knutson, B. L.; Rankin, S. E. *Langmuir* **2004**, *20*, 6981.
(8) Rankin, S. E.; Tan, B.; Lehmler, H.-J.; Hindman, K. P.; Knutson, B. L. *Microporous Mesoporous Mater.* **2004**, *73*, 197.
(9) Blin, J. L.; Lesieur, P.; Stebe, M. J. *Langmuir* **2004**, *20*, 491.
(10) Meng, X.; Di, Y.; Zhao, L.; Jiang, D.; Li, S.; Xiao, F.-S. *Chem. Mater.* **2004**, *16*, 5518.
(11) Tan, B.; Lehmler, H.-J.; Vyas, S. M.; Knutson, B. L.; Rankin, S. E. *Chem. Mater.* **2005**, *17*, 916.
(12) Tan, B.; Lehmler, H.-J.; Vyas, S. M.; Knutson, B. L.; Rankin, S. E. *Adv. Mater.* **2005**, *17*, 2368.
(13) Osei-Prempeh, G.; Lehmler, H. J.; Knutson, B. L.; Rankin, S. E. *Microporous Mesoporous Mater.* **2005**, *85*, 16.
(14) Ghosh, K.; Lehmler, H. J.; Rankin, S. E.; Knutson, B. L. *Langmuir* **2005**, *21*, 6145.
(15) Luzzati, V.; Tardieu, A.; Gulik-Krzywicki, T. *Nature (London)* **1968**, *217*, 1028.
(16) Hyde, S. T. *Current Opin. Colloid Interface Sci.* **1996**, *1*, 653.
(17) Vartuli, J. C.; Schmitt, K. D.; Kresge, C. T.; Roth, W. J.; Leonowicz, M. E.; McCullen, S. B.; Hellring, S. D.; Beck, J. S.; Schlenker, J. L.; Olson, D. H.; Sheppard, E. W. *Chem. Mater.* **1994**, *6*, 2317.
(18) Peña, M. L.; Kan, Q.; Corma, A.; Rey, F. *Microporous Mesoporous Mater.* **2001**, *44−45*, 9.
(19) Asakawa, T.; Hisamatsu, H.; Miyagishi, S. *Langmuir* **1995**, *11*, 8.
(20) Sayari, A.; Kruk, M.; Jaroniec, M. *Catal. Lett.* **1997**, *49*, 147.
(21) Grün, M.; Unger, K. K.; Matsumoto, A.; Tsutsumi, K. *Microporous Mesoporous Mater.* **1999**, *27*, 207.
(22) Han, Y.; Ying, J. Y. *Angew. Chem., Int. Ed.* **2005**, *44*, 288.

(23) Zhao, D.; Huo, Q.; Feng, J.; Kim, J.; Han, Y.; Stucky, G. D. *Chem. Mater.* **1999**, *11*, 2668.
(24) Sing, K. S. W.; Everett, D. H.; Hual, R. A. W.; Moscou, L.; Pierottic, R. A.; Rouquérol, J.; Siemieniewska, T. *Pure Appl. Chem.* **1985**, *57*, 603.
(25) Tan, B.; Rankin, S. E. *J. Phys. Chem. B* **2004**, *108*, 20122.
(26) Wang, K.; Karlsson, G.; Almgren, M.; Asakawa, T. *J. Phys. Chem. B* **1999**, *103*, 9237.
(27) Giulieri, F.; Krafft, M.-P. *Colloids Surf., A* **1994**, *84*, 121.
(28) Israelachvili, J. N.; Mitchell, D. J.; Ninham, B. W. *J. Chem. Soc., Faraday Trans. 2* **1976**, *72*, 1525.
(29) Bernal, J. D.; Fankuchen, I. *J. Gen. Physiol.* **1941**, *25*, 111.
(30) Hohenberg, P. C.; Swift, J. B. *Phys. Rev. E* **1995**, *52*, 1828.
(31) Wulff, G. *Z. Kristallogr.* **1901**, *34*, 449.
(32) Prinsen, P.; van der Schoot, P. *Phys. Rev. E* **2003**, *68*, 021701.
(33) Fournier, J. B.; Durand, G. *J. Phys. II France* **1991**, *1*, 845.
(34) Rankin, S. E.; Tan, B.; Lehmler, H.-J.; Knutson, B. L. *Mater. Res. Soc. Symp. Proc.* **2003**, *775*, 47.